ORIGINAL PAPER

COMPUTATIONAL CHARACTERIZATION OF COMPOUNDS WITH ANTI-MELANOMA ACTIVITY ON THE SK-MEL-5 CELL LINE

EMILIA AMZOIU[1], DENISA AMZOIU[1*], GABRIELA RAU[1], SOFIA POPESCU[2], MARIA VIORICA CIOCILTEU[1], SAMIR ABOU-KHALIL[1], TUDOR TAISESCU[3], ALEXANDRU CHELU[3], OANA TAISESCU[3]

Manuscript received: 02.11.2025; Accepted paper: 18.12.2025;
Published online: 30.12.2025.

Abstract. *Malignant melanoma remains one of the most aggressive forms of skin cancer, underscoring the need for improved therapeutic strategies. In this study, a computational approach combining Quantitative Structure–Activity Relationship (QSAR) analysis and molecular docking was employed to investigate the molecular determinants of anticancer activity against the human melanoma cell line. A set of ten drug molecules with reported growth inhibition data (pGI_{50}) was selected for analysis. QSAR analysis revealed that both geometric parameters and frontier molecular orbital descriptors significantly influence biological activity, highlighting the importance of molecular size, flexibility, and electron-donating/accepting capabilities. Molecular docking simulations were subsequently performed against the target protein associated with the SK-MEL-5 cell line (PDB ID: 3OG7) to evaluate binding affinity and interaction patterns. The docking results showed distinct differences in binding energies and interaction profiles among the compounds, with methotrexate, rhodomycin A, and triazinate exhibiting the most favorable binding characteristics. Overall, the integrated QSAR and docking approach provides mechanistic insight into ligand–receptor interactions and supports the rational interpretation of structure–activity relationships in melanoma.*

Keywords: *SK-MEL-5; QSAR; molecular docking.*

1. INTRODUCTION

Malignant melanoma is one of the most aggressive forms of skin cancer, characterized by rapid progression, high metastatic potential, and resistance to conventional therapies. Despite advances in targeted and immunotherapies, melanoma remains associated with significant morbidity and mortality, highlighting the need for continued discovery and optimization of novel anticancer agents. In this context, human melanoma cell lines, such as SK-MEL-5, play a crucial role in preclinical drug evaluation and mechanistic studies.

The SK-MEL-5 cell line, derived from metastatic human melanoma, is widely used as a representative in vitro model for assessing anticancer activity due to its well-characterized genetic background and reproducible response to cytotoxic and targeted compounds [1,2].

[1] University of Medicine and Pharmacy of Craiova, Faculty of Pharmacy, 200349 Craiova, Romania.
E-mail: emilia.amzoiu@umfcv.ro; denisa.amzoiu@umfcv.ro; gabriela.rau@umfcv.ro; maria.ciocilteu@umfcv.ro; samir.abou-khalil@live.com.
[2] Banat's University of Agriculture Science and Veterinary Medicine, 300645 Timisoara, Romania.
E-mail: sofiapopescu@yahoo.com.
[3] University of Medicine and Pharmacy of Craiova, Faculty of Medicine, 200349 Craiova, Romania.
E-mail: taisescu@gmail.com; mihai.alex170@yahoo.com; oana.taisescu@umfcv.ro.
[*] *Corresponding author: denisa.amzoiu@umfcv.ro.*

https://doi.org/10.46939/J.Sci.Arts-25.4-b01

This cell line is frequently included in large-scale screening programs, such as the NCI-60 panel, making it a valuable benchmark for correlating molecular properties with biological activity.

To complement experimental approaches, Quantitative Structure–Activity Relationship (QSAR) methods have emerged as powerful computational tools for predicting biological activity based on molecular structure. QSAR techniques are based on physicochemical, electronic, and steric descriptors to establish mathematical models that relate chemical structure to pharmacological effects [3,4]. These models reduce experimental costs, accelerate lead optimization, and provide insight into the molecular determinants governing anticancer activity, including those relevant to melanoma cells such as SK-MEL-5.

In parallel, molecular docking has become an essential technique for exploring ligand–receptor interactions at the atomic level. Docking simulations enable the prediction of binding modes, interaction energies, and key amino acid residues involved in molecular recognition, offering mechanistic explanations for observed biological activities [5,6]. When combined with QSAR analysis, docking provides complementary structural validation of predictive models and helps identify favorable interaction patterns within biological targets relevant to cancer progression.

The integration of QSAR modeling and molecular docking, therefore, represents a robust computational strategy for understanding structure–activity relationships and guiding the rational design of new anticancer agents. In this study, computational methods are applied to analyze compounds exhibiting activity against the SK-MEL-5 melanoma cell line, with the aim of elucidating the molecular features governing their biological effects and supporting future drug development efforts.

2. MATERIALS AND METHODS

A computational chemical modeling study was performed on ten drug molecules using the HyperChem software package (HyperCube Inc., Gainesville, FL, USA) [7]. Initially, two-dimensional (2D) molecular structures of the investigated compounds were constructed and subsequently converted into three-dimensional (3D) models within the HyperChem environment. Geometry optimization was carried out using two complementary approaches: molecular mechanics employing the MM+ force field and semi-empirical quantum chemical calculations based on the PM3 method, both implemented in HyperChem version 8.0.8 [7].

Energy minimization was achieved using the Polak–Ribiere conjugate gradient algorithm, with a root mean square (RMS) gradient convergence criterion set to 0.1 kcal/(Å·mol). These optimized geometries were further used to calculate physicochemical and electronic descriptors within the Quantitative Structure–Activity Relationship (QSAR) module of HyperChem. The computed parameters provide insights into the compounds' structural features, their potential interactions with biological membranes, and their predicted pharmacokinetic behavior.

Molecular docking simulations were conducted to investigate the binding interactions between the optimized ligands and the receptor active sites using the HEX docking program (version 8.0.0) [8]. A standard docking protocol was applied, employing the "Shape + Electro" correlation mode to account for both steric complementarity and electrostatic interactions between ligands and receptors. For each docking run, the top 100 binding poses were generated and ranked according to their docking energy scores.

Prior to docking, HEX automatically removed all crystallographic water molecules and non-relevant heteroatoms from the receptor structures. Each protein was then re-centered at the coordinate origin, and intermolecular separations were evaluated as part of the docking

process. Docking scores were calculated for all generated orientations, and the highest-ranking conformations were retained. The resulting docking poses were visually inspected, and the most energetically favorable and sterically plausible complexes were selected for detailed analysis.

The three-dimensional structures of the receptor proteins used in this study were retrieved from the Protein Data Bank [9].

3. RESULTS AND DISCUSSION

In the present study, a set of ten drug molecules was selected for computational analysis to investigate the relationship between molecular structure and anticancer activity against the SK-MEL-5 melanoma cell line. These compounds were chosen based on the availability of experimentally determined growth inhibition data (pGI_{50}) and their structural diversity, which allows for a meaningful exploration of structure–activity relationships [10]. The optimized molecular structures of the selected drugs are presented alongside their corresponding pGI_{50} values, providing a comparative framework for evaluating how specific physicochemical and electronic features influence biological activity (Table 1). This integrated analysis provides the basis for subsequent QSAR modeling and molecular docking studies aimed at elucidating the molecular determinants underlying the observed anticancer effects.

Table 1. Compounds studied and pGI50 anticancer activity on the melanoma cell line SK-MEL-5 [11]

Code	Compound		pGI_{50}
1	Deoxydoxorubicin	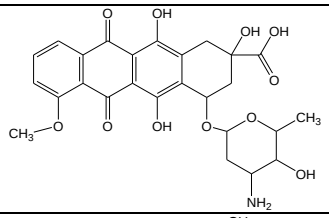	7.602
2	Rhodomycin A	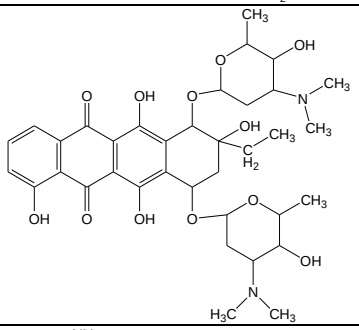	7.491
3	9-Aminocamptothecin	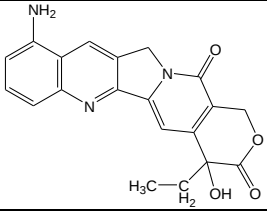	7.594
4	Camptothecin, N,N-Dimethyl Glycinate	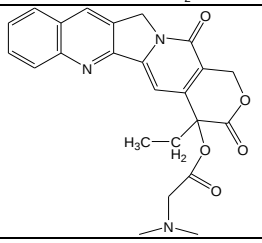	7.504

5	Camptothecin	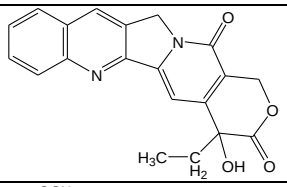	7.561
6	9-Methoxycamptothecin	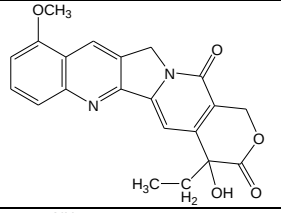	7.641
7	Triazinate	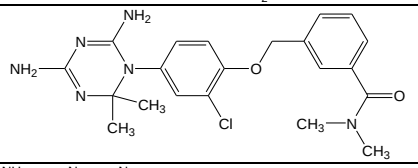	7.170
8	Methotrexate	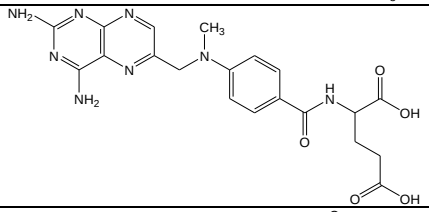	7.024
9	3-Demethylthiocolchicine	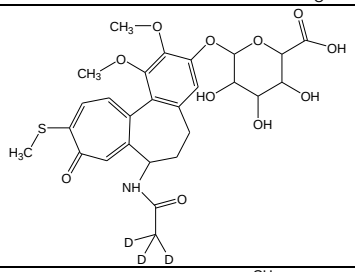	7.810
10	N-Benzoyl-deacetylcolchicine	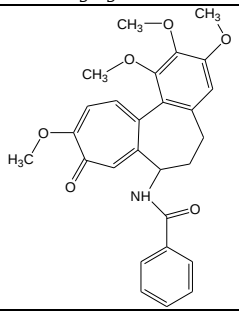	7.969

The 2D structures of the studied compounds were converted into three-dimensional structures using HyperChem 8.0 [7].

The physicochemical parameters calculated in this study encode both electronic and geometric aspects of the analyzed compounds (Tables 2a and b). The presence of these descriptors reflects the role of steric and electronic interactions in influencing the anticancer pGI50 activity on the SK-MEL-5 melanoma cell line.

The energy difference ΔE is a molecular descriptor associated with chemical reactivity; the smaller the ΔE value, the higher the reactivity and thus the lower the molecular stability.

It is notable that compounds **2**, **3**, **4**, and **5** display approximately the same ΔE value; their occupied (HOMO) and unoccupied (LUMO) energy levels are very close due to strong electronic conjugation. As a result, the energy required for the HOMO → LUMO electronic transition is minimal [12]. In compound **2**, electronic conjugation is weakest, which explains its higher ΔE relative to the other three molecules.

Table 2a. The physicochemical parameters calculated by HyperChem 8.0

Compound	SA, A^2	V, A^3	E_h [kcal/mol]	logP	R_M, A^3	α,A^3
1	544.66	1291.69	-25.69	-2.95	133.55	50.17
2	716.37	1664.67	-19.53	-2.36	174.47	66.61
3	408.05	952.84	-12.91	-2.41	104.12	37.53
4	533.07	1147.16	-5.58	-0.69	123.15	44.96
5	408.66	924.05	-8.60	-0.69	100,57	36.18
6	459.4	997.5	-9.32	-1.68	106.95	38.66
7	585.98	1195.03	-12.18	0.45	125.48	45.76
8	593.52	1246.79	-29.48	-1.45	120.24	45.06
9	662.9	1457.37	-20.80	-2.22	149.94	56.26
10	556.22	1238.52	-8.86	-1.50	138.53	49.57

SA – Surface Area; V – Volume; E_h – Hydration Energy; R_M – molar refractivity; α – Polarizability

Table 2b. The physicochemical parameters calculated by HyperChem 8.0

Compound	E_{HOMO} [eV]	E_{LUMO} [eV]	ΔE [eV]	λ [eV]	η [eV]
1	-9.136	-1.079	8.057	5.1075	4.0285
2	-8.660	-1.071	7.589	4.8655	3.7945
3	-8.920	-1.559	7.361	5.2395	3.6805
4	-9.058	-1.558	7.500	5.3080	3.7500
5	-9.103	-1.585	7.518	5.3440	3.7590
6	-9.068	-1.538	7.530	5.3030	3.7650
7	-8.624	-0.561	8.063	4.5925	4.0315
8	-8.814	-1.053	7.761	4.9335	3.8805
9	-8.760	-0.820	7.940	4.7900	3.9700
10	-9.045	-0.561	8.484	4.8030	4.2420

$\Delta E = E_{LUMO} - E_{HOMO}$; λ – absolute electronegativity; η - absolute hardness

Generally, the actual interactions between molecules and their biological receptor—responsible for the onset of biological activity—are preceded by the steric accommodation of the ligand within the receptor's active site.

This accommodation depends on molecular geometry; the larger and less flexible the molecule relative to the active site, the weaker the interaction. This is the case for molecule **2** (Rhodomycin A), which shows the highest values for SA, V, RM, and α, yet does not exhibit the highest anticancer activity (7.491) compared to compound **10**, which shows the strongest anti-melanoma effect (7.969).

N-Benzoyl-deacetylcolchicine (compound 10) has the highest values of ΔE and η, indicating that it is the most stable of the compounds studied and offers the greatest resistance to changes in electron density within the molecular system.

For the camptothecin derivatives, i.e., 9-aminocamptothecin (**3**), camptothecin N-dimethyl glycinate (**4**), and 9-methoxycamptothecin (**6**), most physicochemical properties follow the increasing trend **3** < **6** < **4**, which is consistent with the variation in their molar masses.

In the following sections, the anticancer activity of the studied substances will be analyzed using atomic electronegativity fingerprint descriptors. These descriptors enable the determination of the contribution and role of individual atomic species within each molecule in shaping the biological response. The electronegativity descriptors were calculated using the Elwindow program (original software) from the MOPAC output files [13]. The resulting descriptors are presented in Tables 3a and b.

Table 3a. The electronegativity fingerprint descriptors for HOMO molecular states

Compound	HEL	HELH	HEC	HEO	HEN
1	6.350	0.073	4.804	1.473	0.000
2	6.304	0.071	4.736	1.493	0.004
3	6.106	0.295	3.635	0.721	1.456
4	6.090	0.294	3.640	0.706	1.449
5	6.123	0.306	3.670	0.720	1.427
6	6.106	0.295	3.635	0.721	1.456
7	6.254	0.109	0.720	0.000	5.422
8	6.723	0.110	1.882	0.000	4.731
9	6.040	0.000	2.247	0.088	0.000
10	6.172	0.153	5.188	0.818	0.012

Table 3b. The electronegativity fingerprint descriptors for LUMO molecular states

Compound	LEL	LELH	LEC	LEO	LEN
1	6.051	0.041	5.212	0.798	0.000
2	6.234	0.036	5.215	0.983	0.000
3	6.196	0.082	4.613	0.027	1.474
4	6.238	0.077	4.583	0.033	1.545
5	6.244	0.071	4.579	0.026	1.568
6	6.196	0.082	4.613	0.027	1.474
7	6.044	0.006	5.895	0.043	0.023
8	6.696	0.089	2.770	0.000	3.837
9	5.717	0.000	5.544	0.022	0.000
10	6.072	0.047	5.874	0.143	0.008

The statistical correlation of these descriptors with drug activity was performed using Excel [14]. The values of the correlation coefficients R^2 [%] for atoms are summarized in Table 4.

Table 4. Correlation coefficients R^2 [%] for the electronegativity of molecular states.

Atom	HOMO	LUMO
H	0.3	3.1
C	42.6	32.6
O	15.2	0.5
N	74.1	31.8

As shown in Table 4, among the atomic species involved, nitrogen atoms in the HOMO/LUMO quantum–molecular states make the most significant contributions, accounting for 74.1% (HEN) and 31.8% (LEN), respectively, while carbon atoms contribute 42.6% (HEC) and 32.6% (LEC) to the HOMO/LUMO states in the generation of the biological response.

The values of the correlation coefficients reported for the HOMO and LUMO states suggest the possibility of electron transfer between nitrogen and carbon atoms in the chemical structures of the studied compounds and atoms located in the active site of the biological receptor, followed by the formation of chemical bonds [15].

In the case of oxygen atoms, the higher correlation coefficient value (R^2 = 15.2%) for the HOMO state indicates a charge transfer from the oxygen atoms of the studied compounds toward the receptor active site.

To identify which nitrogen atoms in methotrexate effectively contribute to the electronegativity of the HOMO molecular state, the *.mno output file obtained from MOPAC quantum–molecular calculations was analyzed. For methotrexate, the HOMO state is described by molecular orbital number 86.

For this molecular orbital, the contributions of the 55 atoms constituting the compound (Fig. 1) are summarized in Table 5. As shown in Table 5, nitrogen atoms 1, 7, 10, and 32 exhibit the highest contributions to the electronegativity of the HOMO state among all atoms in this molecular species.

Such an analysis of the contributions and spatial localization of atomic species opens a new avenue for identifying molecular fragments or chemical groups that play a dominant role in the development of pharmacological activity. The identification of these active regions within chemical structures enables the rational design of new compounds with optimized medicinal activity (Table 5).

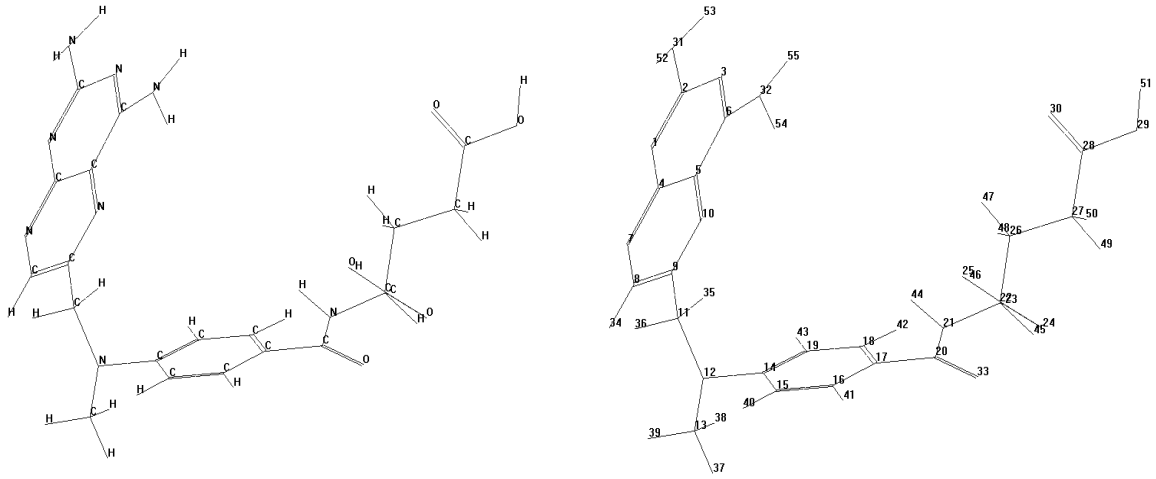

Figure 1. Methotrexate compound and the numbering of its constituent atoms.

Table 5. Contribution of atoms to the HOMO molecular state (MO no. 86) of the methotrexate compound.

1N 0.51518	12N -0.02459	23C 0.00011	34H -0.00193	45H 0.00010
2C 0.18826	13C 0.0110	24O -0.00013	35H 0.00251	46H 0.00003
3N -0.04224	14C -0.01262	25O -0.00011	36H 0.05705	47H 0.00003
4C -0.10570	15C -0.00252	26C 0.00001	37H -0.0128	48H 0.00002
5C -0.40700	16C -0.00328	27C -0.00007	38H 0.00721	49H 0.00001
6C -0.10897	17C 0.00269	28C -0.00001	39H -0.0027	50H -0.00001
7N -0.22118	18C -0.00109	29O -0.00001	40H -0.00104	51H -0.00001
8C 0.03446	19C -0.00348	30O 0.00000	41H -0.00277	52H -0.05738
9C 0.32494	20C -0.00095	31N -0.01332	42H 0.00018	53H -0.06143
10N 0.13498	21N -0.00002	**32N 0.20434**	43H -0.00348	54H 0.04432
11C -0.0470	22C -0.00001	33O 0.00310	44H 0.00004	55H 0.04413

To further understand the electronic features governing the biological activity and binding behavior of the investigated compounds, the spatial distributions of the highest occupied molecular orbital (HOMO) and the lowest unoccupied molecular orbital (LUMO) were analyzed for methotrexate and rhodomycin. Visualization of these frontier molecular orbitals provides insight into potential electron donor and acceptor regions, which are critical for molecular recognition, charge transfer processes, and interactions with biological targets (Fig. 2).

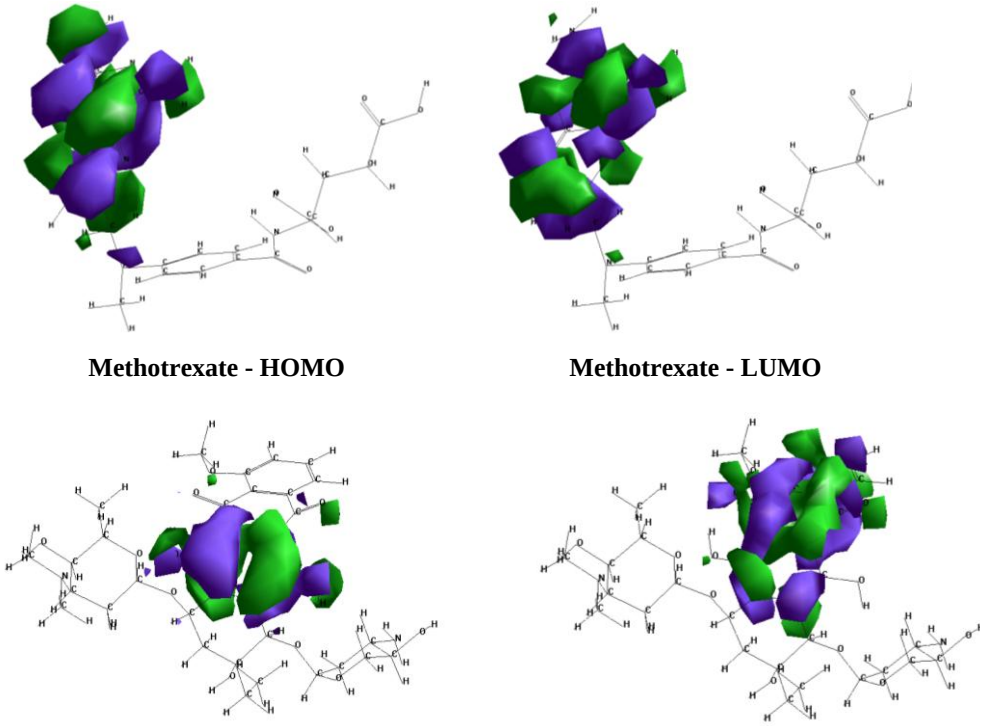

Figure 2. Frontier molecular orbital distributions of the analyzed compounds. The images highlight the spatial localization of electron density associated with the HOMO and LUMO, indicating potential regions involved in electron donation and acceptance during ligand–receptor interactions.

The HOMO and LUMO distributions shown in Figure X reveal distinct electronic characteristics for methotrexate and rhodomycin that may underlie their different biological activities and docking behaviors.

For methotrexate, the HOMO is predominantly localized on heteroatom-rich regions, particularly nitrogen-containing functional groups, indicating a strong potential for electron donation and interaction with electrophilic residues in the receptor binding site. The LUMO, in contrast, is distributed over complementary regions of the molecule, suggesting favorable electron acceptance and participation in charge-transfer interactions [16]. This balanced distribution of frontier orbitals supports the strong binding affinity observed in docking simulations.

In the case of rhodomycin, the HOMO is mainly delocalized over the extended conjugated aromatic system, reflecting enhanced π-electron density and a tendency to engage in π–π stacking and hydrophobic interactions. The LUMO exhibits a broader spatial distribution, which may facilitate interactions with multiple residues but with reduced specificity compared to methotrexate. These electronic features are consistent with its lower, yet still significant, docking energy.

Overall, the comparative HOMO–LUMO analysis highlights how differences in electronic structure influence molecular reactivity and receptor binding. The observed frontier orbital patterns correlate well with docking results and support the role of electron density distribution in modulating ligand–receptor interactions and anticancer activity.

To further elucidate the molecular basis underlying the anticancer activity of the selected compounds, molecular docking studies were subsequently performed between the ten drug molecules and the biological target associated with the SK-MEL-5 melanoma cell line (PDB ID: 3OG7) [17]. Docking simulations were employed to investigate the binding affinity, preferred orientations, and key intermolecular interactions within the active site of the target protein. This approach enables a detailed evaluation of how structural and electronic

features of the ligands influence their accommodation within the binding pocket and contribute to the experimentally observed pGI_{50} values. By correlating docking scores and interaction patterns with biological activity, this step provides mechanistic insight into ligand–receptor recognition and supports the rational interpretation of structure–activity relationships derived from QSAR analysis.

The docking energies presented in Table 6 reflect the predicted binding affinities of the ten investigated compounds toward the selected molecular target associated with the SK-MEL-5 melanoma cell line (PDB ID: 3OG7) [17]. More negative docking energy values indicate stronger and more favorable ligand–receptor interactions, suggesting a higher likelihood of biological activity.

Table 6. The docking results of the binding energies with SK-MEL-5 Cell Line [8].

Compound	Energy [kcal/mol]
Methotrexate	-563.78
Rhodomycin A	-387.66
Triazinate	-363.5
3-Demethylthiocolchicine	-360.98
Deoxydoxorubicin	-333.87
Camptothecin, N,N-Dimethyl Glycinate	-318.2
N-Benzoyl-deacetylcolchicine	-315.88
9-Methoxycamptothecin	-303.37
Camptothecin	-294.31
9-Aminocamptothecin	-291.97

Among the analyzed compounds, methotrexate exhibited the most favorable binding energy (−563.78 kcal/mol), indicating a strong interaction with the receptor active site. This result is consistent with methotrexate's well-established antineoplastic activity and its capacity to form multiple stabilizing interactions, including hydrogen bonds and electrostatic contacts, within the binding pocket. Rhodomycin A also showed a highly favorable docking score (−387.66 kcal/mol), likely attributable to its extended conjugated system and multiple functional groups capable of interacting with key amino acid residues.

Intermediate binding affinities were observed for triazinate, 3-demethylthiocolchicine, and deoxydoxorubicin, with docking energies ranging from −363.50 to −333.87 kcal/mol. These compounds present a balance between molecular size, flexibility, and functional group distribution, which appears to support stable binding while avoiding excessive steric hindrance.

The camptothecin derivatives demonstrated comparatively lower binding affinities, with docking energies between −318.20 and −291.97 kcal/mol. Among these, Camptothecin N,N-dimethyl glycinate, and N-benzoyl-deacetylcolchicine showed slightly improved binding relative to the parent camptothecin, suggesting that structural modifications may enhance receptor interactions. In contrast, 9-aminocamptothecin exhibited the least favorable docking energy, possibly due to reduced complementarity with the active site or suboptimal orientation within the binding pocket.

Overall, the docking results reveal a clear differentiation in binding propensity among the tested compounds and provide mechanistic insight into their potential anticancer activity. The observed trends support the notion that both molecular size and the presence of functional groups capable of forming strong intermolecular interactions play critical roles in stabilizing ligand–receptor complexes [18]. When considered alongside pGI_{50} values and QSAR descriptors, these findings contribute to a more comprehensive understanding of the structure–activity relationships governing anticancer effects in the SK-MEL-5 melanoma model.

Fig. 3 illustrates the binding interactions of the three highest-ranked compounds—methotrexate, rhodomycin A, and triazinate—within the active site of the SK-MEL-5 target protein (PDB ID: 3OG7). The 3D representations highlight the spatial orientation of each ligand and its overall fit within the receptor pocket, emphasizing steric complementarity and molecular accommodation [19]. Complementary 2D projections depict the specific amino acid residues involved in key interactions, including hydrogen bonding, hydrophobic contacts, and electrostatic stabilization [20]. Together, these visualizations provide a comprehensive understanding of the molecular determinants governing ligand binding and offer mechanistic insight into the observed differences in docking energies among the compounds.

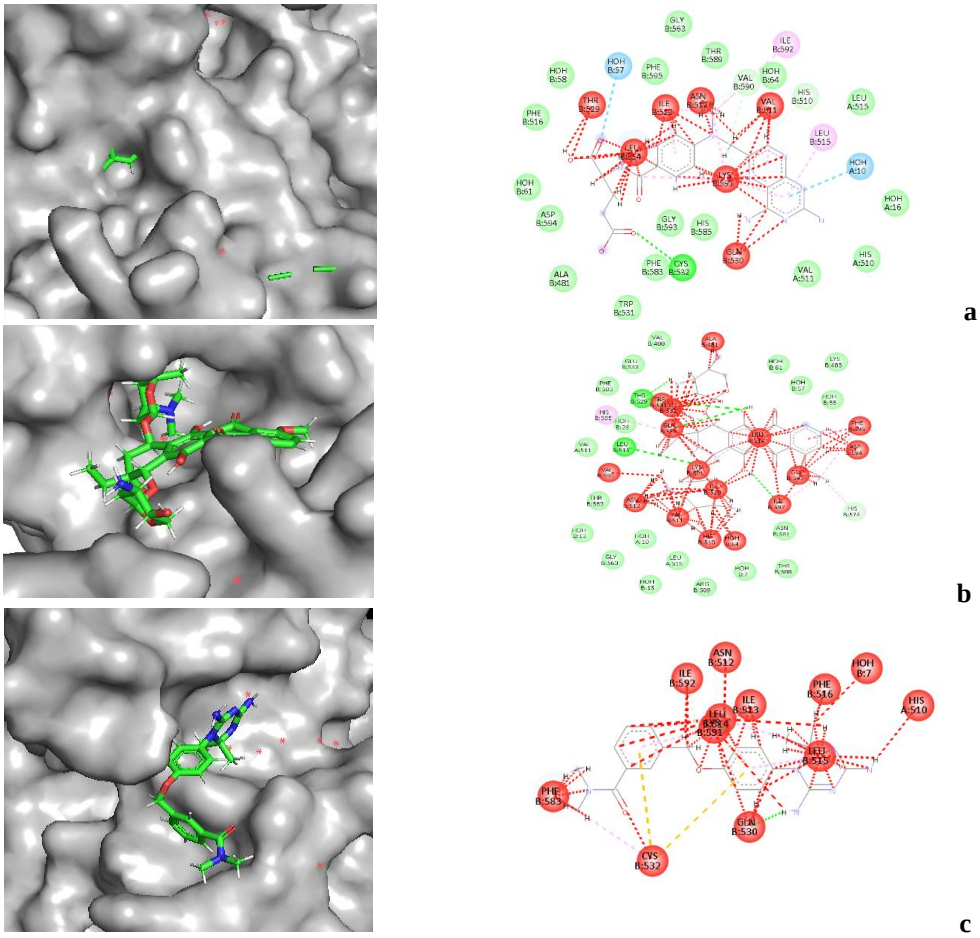

Figure 3. Binding interactions of the top three compounds with the SK-MEL-5 target protein (PDB ID: 3OG7): a) Methotrexate; b) Rhodomycin A; c) Triazinate. The figure presents 3D representations of the ligand orientations within the active site alongside 2D projections, highlighting the key amino acid residues involved in hydrogen bonding, hydrophobic, and electrostatic interactions [19, 20].

The 3D and 2D visualizations of methotrexate, rhodomycin A, and triazinate within the SK-MEL-5 target protein (PDB ID: 3OG7) provide detailed insight into the molecular interactions underlying their predicted binding affinities [21].

Methotrexate (A) demonstrates the most extensive network of stabilizing interactions, forming multiple hydrogen bonds and electrostatic contacts with key residues in the active site [22]. Its orientation fully occupies the binding pocket, allowing optimal steric complementarity, which is consistent with its most favorable docking energy (−563.78 kcal/mol).

Rhodomycin A (B) also shows strong binding, with hydrogen bonds and hydrophobic contacts distributed along its extended conjugated structure. While its docking energy (−387.66 kcal/mol) is lower than that of methotrexate, the 3D representation highlights its

ability to engage multiple subpockets within the receptor, supporting its potential biological activity.

Triazinate (C) occupies a smaller volume of the active site and forms fewer stabilizing contacts, consistent with its higher (less favorable) docking energy (−363.50 kcal/mol). Its interactions are primarily limited to key polar and aromatic residues, suggesting that its binding is less extensive but still significant.

Overall, the combination of 3D orientation and 2D interaction mapping allows for a detailed assessment of the steric and electronic factors contributing to ligand–receptor recognition [23-25]. The figure illustrates that binding affinity is influenced not only by the number and type of interactions but also by how well each compound fits into the receptor's active site, providing mechanistic insight into the observed differences in docking energies and potential anticancer activity.

It should be emphasized that the present study is based entirely on theoretical and computational approaches, including QSAR modeling and molecular docking simulations [26]. While these methods provide valuable predictive insight into structure–activity relationships and ligand–receptor interactions, they inherently rely on approximations and assumptions regarding molecular behavior in biological environments [27]. Consequently, the predicted binding affinities, interaction patterns, and electronic properties may not fully capture the complexity of real biological systems, such as protein flexibility, solvent effects, metabolic transformations, and cellular context.

In vitro assays using the SK-MEL-5 melanoma cell line, followed by *in vivo* studies, are necessary to verify the predicted anticancer activity, binding mechanisms, and safety profiles of the investigated compounds [28]. Despite these limitations, the present theoretical study provides a rational framework for prioritizing candidates and guiding future experimental investigations, thereby reducing time and costs associated with drug discovery and optimization.

4. CONCLUSIONS

The QSAR analysis provided valuable insight into the relationship between molecular structure and anticancer activity against the SK-MEL-5 melanoma cell line. The evaluated physicochemical and electronic descriptors highlighted the critical role of both steric and electronic factors in modulating biological response. Parameters related to molecular size, shape, and flexibility influenced ligand accommodation within the biological target, while electronic descriptors, particularly EHOMO, ELUMO, and the HOMO–LUMO energy gap (ΔE), were indicative of molecular reactivity and charge-transfer potential.

The results suggest that compounds exhibiting balanced electronic properties and favorable geometric characteristics are more likely to display enhanced biological activity. The strong contribution of heteroatoms, especially nitrogen and oxygen, to frontier molecular orbitals underscores their importance in mediating interactions with biological receptors. Overall, the QSAR findings complement the molecular docking results and support their combined use as an effective strategy for predicting activity and guiding the rational design of new anticancer agents targeting melanoma.

The molecular docking analysis of the ten selected compounds against the SK-MEL-5 target protein (PDB ID: 3OG7) revealed clear differences in predicted binding affinities and interaction patterns. Methotrexate exhibited the most favorable docking energy, forming extensive hydrogen bonds and electrostatic contacts, followed by Rhodomycin A and Triazinate, which also displayed significant but less extensive interactions.

The results indicate that molecular size, flexibility, and the presence of functional groups capable of forming stabilizing interactions are critical determinants of binding strength. Compounds with optimal steric complementarity and multiple interaction sites achieved higher docking scores, suggesting a correlation between predicted binding affinity and potential anticancer activity. Overall, these findings provide mechanistic insight into the ligand–receptor interactions underlying the observed pGI_{50} values and highlight the utility of combined 3D and 2D docking analyses for evaluating and prioritizing compounds for further experimental investigation.

REFERENCES

[1] Shoemaker, R. H., *Nature Reviews Cancer*, **6**, 813, 2006.
[2] Alley, M. C., Scudiero, D. A., Monks, A., Hursey, M. L., Czerwinski, M. J., Fine, D. L., B. J., Abbott, B. J., Mayo, J. G., et al, *Cancer Research*, **48**, 589, 1988.
[3] Hansch, C., Leo, A., Hoekman, D., *Exploring QSAR: Fundamentals and Applications in Chemistry and Biology*, ACS Publications, Washington, 1995.
[4] Cherkasov, A., Muratov, E. N., Fourches, D., Varnek, A., et al, *Journal of Medicinal Chemistry*, **57**(12), 4977, 2014.
[5] Morris, G. M., Lim-Wilby, M., *Methods in Molecular Biology*, **443**, 365, 2008.
[6] Kitchen, D. B., Decornez, H., et al, *Nature Reviews Drug Discovery*, **3**(11), 935, 2004.
[7] HyperChem Professional Release 8. www.hyper.com
[8] https://hex.loria.fr
[9] https://www.rcsb.org
[10] Amzoiu, E., Amzoiu, M. O., Anoaica, P. G., *Revue Roumaine de Chimie*, 54, 671, 2009.
[11] Umar, A. B., Uzairu, A., Shallangwa, G. A., Uba, S., *SN Applied Sciences*, **2**, 815, 2020.
[12] Anoaica, P. G., Amzoiu, E., Bozzini, F., et al, *Revue de Chimie*, **66**, 390, 2015.
[13] MOPAC 2007, JJP Stewart, Stewart Computational Chemistry, Colorado Springs, CO, USA, http://openMOPAC.net 2007. http://openmopac.net/
[14] https://www.microsoft.com/ro-ro/microsoft-365/excel
[15] Rezvan, V. H., *Results in Chemistry*, **7**, 101437, 2024.
[16] Anoaica, P. G., Amzoiu, E., Lepădatu, C., *Revue Roumaine de Chimie*, **52**, 789, 2007.
[17] Bollag, G., Hirth, P., Tsai, J., Zhang, J., Ibrahim, P. N., et al., *Nature*, **467**, 596, 2010.
[18] Amzoiu, D., Stoian, A. M., Amzoiu, E., Rau, G., *Revue de Chimie*, **66**, 2013, 2015.
[19] Schrödinger, L., DeLano, W., *PyMOL Molecular Graphics System*, 2020. http://www.pymol.org/pymol
[20] Biovia, D., Berman, H., Westbrook, J., Feng, Z., Gilliland, G., Bhat, T., Richmond, T. J., *Discovery Studio Visualizer*, Dassault Systèmes, San Diego, 2016.
[21] Amzoiu, M.O., Popescu, G. S., Amzoiu, E., Ciocilteu, M. V., et al, *Life*, **15**, 1247, 2025.
[22] Amzoiu, M., Popescu, S., Amzoiu, E., Chelu, A., Ciocilteu, M. V., *Journal of Science and Arts*, **24**, 419, 2024.
[23] Amzoiu, M. O., Taisescu, O., Amzoiu, E., Gresita, A., Popescu, G. S., Rău, G., Ciocilteu, M. V., Manda, C. V., *Life*, **15**, 1903, 2025.
[24] Radulescu C., *Revista de Chimie*, **56**(2), 151, 2005.
[25] Radulescu C., Tarabasanu-Mihaila C., *Rev. de chimie* (Bucharest), **55**(1), 25, 2004.
[26] Amzoiu, M., Amzoiu, E., Belu, I., Popescu, S., Cheita, G., Amzoiu, D., *Journal of Science and Arts*, **2**, 469, 2019.
[27] Tian, Y. Y., Tong, J. B., Liu, Y., Tian, Y., *Molecules*, **29**, 1772, 2024.
[28] Amzoiu, M., Chelu, A., Popescu, S., Amzoiu, E., Ciocilteu, M., *Journal of Science and Arts*, **23**, 1009, 2023.